Preparation and Performance of Silica Membranes on α-Alumina Flat Disk for Bio-CNG (CH_4/CO_2) Purification

R Dirja[1]*, J K Putri[1], Suprihatin[1], H Saputra[2], A Andini[2], and Arfiana[2]

[1] Department of Chemical Engineering, Faculty of Engineering and Science, Universitas Pembangunan Nasional "Veteran" Jawa Timur, Surabaya, Indonesia
[2] National Research and Innovation Agency, Jakarta, Indonesia

ARTICLE INFO

CORRESPONDING AUTHOR

*E-mail: ramadhanudj@gmail.com

ABSTRACT

This study focuses on the synthesis and performance evaluation of silica membranes supported on α–alumina flat disks for bio–CNG (CO_2/CH_4) purification. The membranes were fabricated via a sol–gel method using tetraethyl orthosilicate (TEOS) as the silica precursor and cetyltrimethylammonium bromide (CTAB) as the templating agent. CTAB concentrations were varied from 0.01 to 0.09 M, while drying temperatures ranged from 80 to 120 °C. Characterisation through SEM–EDX, XRD, and gas permeation tests revealed that an increase in CTAB concentration produced a more uniform pore structure and enhanced CH_4 flux. However, excessive CTAB led to over–templating, resulting in microcracks. The optimal membrane was obtained at 0.05 M CTAB and a drying temperature of 105 °C, yielding a separation factor (α = 2.14) with stable structural integrity. Gas transport was dominated by Knudsen diffusion, favouring CH_4 over CO_2, with an experimental CH_4/CO_2 selectivity (α = 3.21) exceeding the theoretical Knudsen value (1.66). This indicates that, in addition to Knudsen flow, microstructural factors such as pore interconnectivity and partial defects contributed to CH_4 transport through the silica membrane. These findings indicate that silica membranes synthesised under optimised sol–gel conditions exhibit strong potential for efficient bio–CNG upgrading, supporting renewable, low–carbon energy applications.

Contribution to Sustainable Development Goals (SDGs):
SDG 7: Affordable and Clean Energy
SDG 9: Industry, Innovation, and Infrastructure
SDG 13: Climate Action

1. INTRODUCTION

1.1. Research Background

Energy is an essential component supporting activities across all sectors. In Indonesia, energy consumption remains dominated by fossil fuels [1], while national demand continues to rise. According to [2], economic activities account for more than 50% of total CO_2 emissions, emphasizing the urgency of developing low-carbon and renewable energy alternatives. Biogas is one such promising option, as it is produced from biodegradable materials such as livestock waste and Palm Oil Mill Effluent (POME). Typical POME-derived biogas contains 50–75% CH_4, 25–45% CO_2, <2% N_2, 0.1–0.5% H_2S, and trace O_2 [3]. Methane-rich biogas (>40% CH_4) is highly combustible and has substantial calorific value [4], but its CO_2 content still contributes to greenhouse gas emissions.

CO_2 removal is commonly performed using adsorption [5]; however, this method requires continuous adsorbent regeneration, generating secondary waste and increasing chemical use [6]. Membrane-based gas separation offers a sustainable alternative due to its reusability, chemical-free operation, and strong mechanical and thermal stability. Silica

membranes supported on α-alumina are particularly attractive because of their tunable mesoporous structure and robustness. Surfactants such as CTAB are widely used as templating agents, enabling control over pore size and distribution during synthesis. Recent studies highlight the advancement of silica-based membranes. Pizzoccaro-Zilamy et al [7], demonstrated highly porous mesostructures using a Stöber-solution pore-growth approach. Sutrisna et al. [8] reported enhanced CO_2 selectivity in ZIF-8/polysulfone membranes, though thermal instability limits the polymer's applicability. Han et al [9], further developed sol–gel-based mesoporous silica with adjustable architectures for gas separation. Building on these findings, this study synthesizes silica membranes via sol–gel and dip-coating methods using varied CTAB concentrations (0.01–0.09 M) on α-alumina supports. The objective is to obtain controlled mesoporous structures (2–5 nm) and evaluate their CO_2/CH_4 separation performance for bio-CNG upgrading.

1.2. Literature Review

The global shift toward low-carbon energy systems has increased the significance of biogas upgrading technologies, particularly for producing high-purity bio-CNG. Biogas derived from organic waste streams, such as Palm Oil Mill Effluent (POME), provides an abundant and renewable energy source, yet its high carbon dioxide (CO_2) content requires further purification before utilisation. Various separation techniques have been extensively studied, ranging from adsorption and absorption to membrane-based processes. However, differences in efficiency, environmental impact, and operational stability across these technologies necessitate a deeper understanding of the most sustainable and scalable approach. This section reviews the scientific foundation relevant to this study, including biogas composition, existing CO_2 removal methods, membrane technology, silica membrane synthesis, the role of CTAB templating, and the importance of α-alumina support structures.

1.2.1. Biogas Composition and Upgrading Requirements

Biogas is a renewable energy source produced through anaerobic digestion of organic materials, including livestock manure and POME. Its composition typically consists of 50–75% methane (CH_4) and 25–45% CO_2, with small amounts of nitrogen, hydrogen sulfide, and oxygen [3]. Methane is the primary energy carrier in biogas, and concentrations above 40% make it highly combustible, resulting in a significant heating value [4]. However, the substantial CO_2 fraction reduces combustion efficiency and contributes to greenhouse gas emissions when released into the atmosphere. Therefore, CO_2 removal is essential not only to improve biogas quality but also to support environmental sustainability and meet energy standards for bio-CNG applications.

1.2.2. Conventional CO_2 Removal Technologies

Several conventional methods are used for CO_2 separation from biogas, including absorption, adsorption, and cryogenic distillation. Absorption involves dissolving CO_2 in chemical or physical solvents, but often requires high energy for solvent regeneration. Adsorption using solid sorbents is widely implemented due to its simplicity and lower initial cost [5]. However, this method requires frequent regeneration of the adsorbent, resulting in the production of secondary waste and increased chemical consumption over time [6]. Cryogenic processes can achieve high purity but are energy-intensive and unsuitable for small- to medium-scale applications. These limitations highlight the need for alternative separation technologies that are both effective and environmentally sustainable.

1.2.3. Membrane-Based Gas Separation

Membrane-based gas separation has emerged as a promising solution for biogas upgrading due to its modular operation and low chemical dependency. Membranes enable selective transport of gas molecules based on differences in size, diffusivity, or solubility, making them attractive for CH_4/CO_2 separation. Unlike adsorption or absorption, membrane systems operate continuously, reducing maintenance requirements and minimising chemical waste. Inorganic membranes, especially silica membranes, offer superior thermal and chemical stability compared to polymeric membranes, allowing for long-term operation in harsh environments. The gas transport mechanisms in mesoporous silica membranes are primarily governed by Knudsen diffusion, making them suitable for separating gases with different molecular weights. These characteristics collectively demonstrate the potential of membrane technology as a sustainable alternative for biogas purification.

1.2.4. Silica Membrane Synthesis and The Role of CTAB

Silica membranes synthesized via the sol–gel method have gained attention because the process enables precise control over pore size and structure. During synthesis, the incorporation of surfactants, such as cetyltrimethylammonium bromide (CTAB), serves as a templating agent that directs the formation of ordered mesopores. CTAB micelles facilitate uniform pore development by guiding the assembly of silica species during hydrolysis and condensation reactions. Variations in CTAB concentration directly affect pore size, distribution, and interconnectivity, influencing both permeability and selectivity. Recent studies by Pizzoccaro-Zilamy [7], Sutrisna et al. [8], and Han et al. [9] emphasise the importance of templating strategies to enhance membrane performance, demonstrating that a controlled pore architecture is critical for achieving efficient CO_2/CH_4 separation.

1.2.5. α-Alumina as a Support for Silica Membrane

α-Alumina is widely used as a support material for inorganic membranes due to its outstanding mechanical strength and high temperature stability. Its porous structure provides an ideal foundation for silica layers, enabling strong interfacial adhesion during the sol–gel dip-coating process. The thermal and chemical resistance of α-alumina ensures that the membrane maintains integrity during drying, calcination, and gas permeation operations. These characteristics reduce the likelihood of cracking, a common challenge in unsupported silica membranes. Additionally, the uniform pore distribution in α-alumina supports contributes to stable gas transport pathways, enhancing overall membrane performance. Therefore, α-alumina serves as an essential structural component in the fabrication of durable and high-selectivity silica membranes.

1.2.6. Research Gap and Foundation for This Study

Despite significant advancements in membrane-based gas separation, several gaps remain in the understanding of silica membrane synthesis, particularly regarding the influence of CTAB concentration. Many earlier studies explored polymeric membranes or silica structures synthesized using alternative templating routes, leaving limited insights into CTAB-modified sol–gel membranes on α-alumina flat disk supports. Additionally, inconsistencies in pore structure uniformity and membrane stability across different synthesis methods highlight the need for more systematic investigation. This study addresses these gaps by evaluating silica membranes fabricated with CTAB concentrations ranging from 0.01 to 0.09 M and varying drying temperatures. The performance of these membranes is assessed through SEM–EDX, XRD, and gas permeation tests to identify the optimal synthesis conditions. The findings aim to advance the development of efficient membrane materials for bio-CNG upgrading and support broader renewable energy applications.

1.3. Research Objective

This study aims to evaluate the synthesis parameters of silica membranes, particularly the variation of CTAB concentration and drying temperature, and to analyze their effects on pore structure formation, membrane morphology, and CH_4/CO_2 separation performance for bio-CNG upgrading applications.

2. MATERIALS AND METHODS

This research was carried out at the Laboratory of Energy Resources and Chemical Industry, National Research and Innovation Agency (BRIN), from January 13 to February 20, 2025. The selection of this laboratory was purposive, as BRIN provides comprehensive facilities for sol–gel synthesis, dip-coating deposition, calcination, and membrane characterisation, including SEM–EDX, XRD, and gas permeation testing. These instruments were essential for supporting the fabrication and performance evaluation of silica membranes for CH_4/CO_2 separation in bio-CNG upgrading applications. The primary materials used in this study included TEOS (Tetraethyl orthosilicate) as the silica precursor, hydrochloric acid (HCl) as the acidic catalyst, CTAB as a cationic surfactant and structure-directing agent, ethanol as the reaction medium, aquadest, and α-alumina flat disks as membrane supports. The CTAB concentrations (0.01–0.09 M) were intentionally varied to investigate their effects on pore formation, structural uniformity, and membrane stability. The α-alumina support was chosen for its excellent mechanical strength and thermal resistance, both of which are necessary for producing durable inorganic membranes.

The research method employed an experimental laboratory approach using sol–gel synthesis and dip-coating techniques. The silica sol was prepared by mixing TEOS, ethanol, aquadest, and HCl, followed by the addition of CTAB at predetermined concentrations. The α-alumina supports were coated by dip-coating to ensure uniform deposition of the silica layer. Drying temperatures between 80–120 °C were applied to study their influence on silica network formation, and calcination was performed to remove residual surfactant and stabilize the membrane. Characterisation included SEM–EDX to observe surface morphology and elemental distribution, XRD to analyze structural phases, and gas permeation tests to evaluate CH_4 and CO_2 flux and selectivity. The resulting data were analyzed descriptively to determine the relationship between synthesis parameters and membrane performance, thereby identifying optimal conditions for effective bio-CNG purification.

3. RESULT AND DISCUSSION

3.1. Morphological Analysis of Silica Membranes (SEM-EDX)

The surface morphology and elemental composition of the silica membranes were examined by Scanning Electron Microscopy combined with Energy Dispersive X-ray (SEM–EDX). Representative samples with CTAB concentrations of 0.01 M, 0.05 M, and 0.09 M at a drying temperature of 120 °C were selected to evaluate the influence of surfactant concentration on pore structure and elemental uniformity.

As shown in Figure 1–3, the SEM micrographs exhibit distinct morphological transitions corresponding to CTAB variation. At 0.01 M CTAB, the membrane surface appeared compact and dense, with fewer dark regions, indicating limited micelle formation and minimal pore generation. Increasing the concentration to 0.05 M yielded a more homogeneous surface with evenly distributed micropores, suggesting optimal micelle templating during sol–gel growth. At 0.09 M CTAB, excessive surfactant caused aggregation and irregular pore clusters, reflecting an overtemplating phenomenon that produced local structural collapse. The EDX elemental mapping confirmed the presence of Si, Al, and Zr across all samples. Aluminum and zirconium peaks originated from the α–alumina substrate, while silicon peaks represented the silica top layer. The Si distribution at 0.01 M CTAB was relatively sparse, but it increased significantly at 0.05 M and 0.09 M concentrations, confirming enhanced silica deposition on the substrate. However, the non-uniform coverage at 0.09 M indicated diffusion limitations in the sol phase due to the high viscosity at elevated CTAB concentrations, which restricted penetration during dip-coating [10], [11].
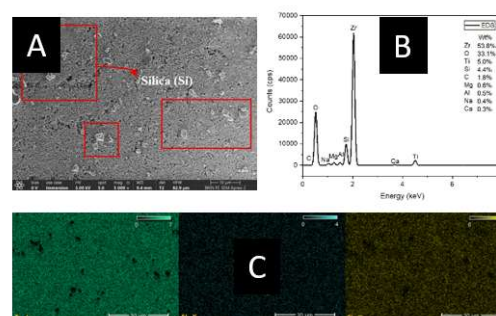

Fig. 1. (A) SEM Test Results; (B) EDX Mapping Results Graph; (C) EDX Mapping Results (Zr, Al, Si) for CTAB Concentration Variation 0.01 M at Drying Temperature 120°C

Fig. 2. (A) SEM Test Results; (B) EDX Mapping Results Graph; (C) EDX Mapping Results (Zr, Al, Si) for CTAB Concentration Variation 0.05 M at Drying Temperature 120°C

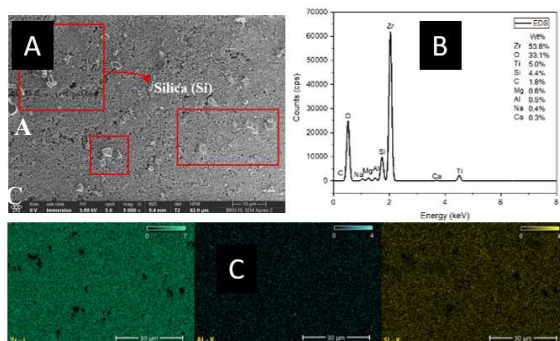

Fig. 3. (A) SEM Test Results; (B) EDX Mapping Results Graph; (C) EDX Mapping Results (Zr, Al, Si) for CTAB Concentration Variation 0.09 M at Drying Temperature 120°C
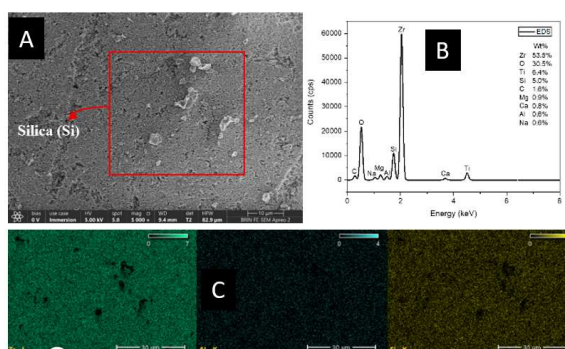
These results indicate that the CTAB concentration critically determines membrane pore formation and surface continuity. An optimal concentration (0.05 M) yielded a mesoporous structure with uniform pore distribution, thereby enhancing gas permeability and selectivity. At higher surfactant levels, the micelle network becomes unstable, leading to random pore aggregation and reduced homogeneity. Similar trends have been reported by Y Gao et al [12] and Kahlib et al. [13], confirming that excessive surfactant disrupts pore symmetry and deteriorates mechanical integrity. Overall, SEM–EDX analysis verifies that the sol–gel synthesis process successfully formed silica membranes with well-distributed Si deposition and strong adhesion to the α–alumina substrate. The optimised CTAB concentration (0.05 M) produced the most homogeneous morphology, which supports the improved gas permeation behaviour observed in subsequent performance testing.

3.2. X-Ray Diffraction (XRD) Analysis

The phase composition and crystallinity of the synthesised silica membranes were analysed by X-ray diffraction (XRD). Figure 4 presents the XRD diffractogram of silica membranes prepared with varying CTAB concentrations at a drying temperature of 120 °C
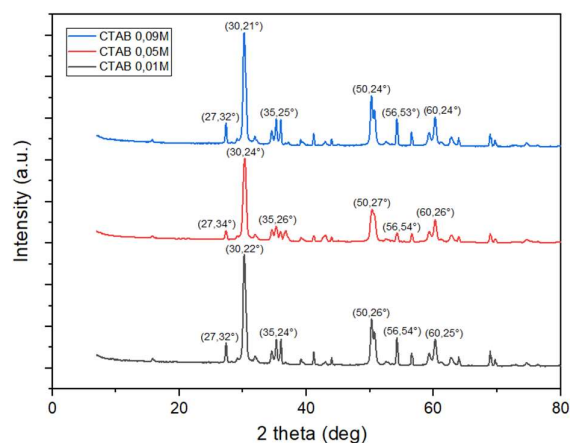

Fig. 4. XRD Intensity Curves of Silica Membranes Sample Variations 0.09M; 0.05M; 0.01M at a Drying Temperature of 120°C

The XRD profiles show a broad diffraction hump at $2\theta = 22°–25°$, corresponding to the amorphous structure of silica (SiO_2). The broad nature of this peak indicates that the membranes predominantly consist of an amorphous silica network formed through sol–gel polymerisation of the TEOS precursor. The absence of sharp diffraction peaks confirms the lack of long-range atomic ordering and demonstrates that the silica structure is mainly composed of randomly oriented Si–O–Si linkages [10], [11]. A slight reflection near $2\theta \approx 27°–28°$ is observed in some samples, suggesting the partial formation of α-quartz crystallites or localized structural ordering at the silica–substrate interface. This minor crystallization likely originates from the thermal treatment process at 120 °C, which promotes densification and condensation of the silica framework [14].

The XRD pattern obtained in this study is consistent with typical amorphous silica structures reported in previous sol–gel based membrane studies [7], [13]. Compared to the reference data by Iqbal et al. [15], the observed hump intensity appears slightly higher, which may be attributed to the influence of the α-alumina substrate and the CTAB templating effect that induce partial organization within the amorphous matrix. Overall, the XRD results confirm that the synthesised silica membranes exhibit predominantly amorphous characteristics, with minor structural ordering. Such a configuration is beneficial for gas separation processes, as it provides sufficient structural stability while maintaining microporous free volume that supports selective diffusion [16].

3.3. Gas Permeation Performance of Silica Membranes

The gas permeation performance of the synthesized silica membranes was evaluated using single-gas permeation tests with CO_2 and CH_4 as feed gases. Measurements were conducted under identical conditions to determine the effects of CTAB concentration on gas flux and selectivity.
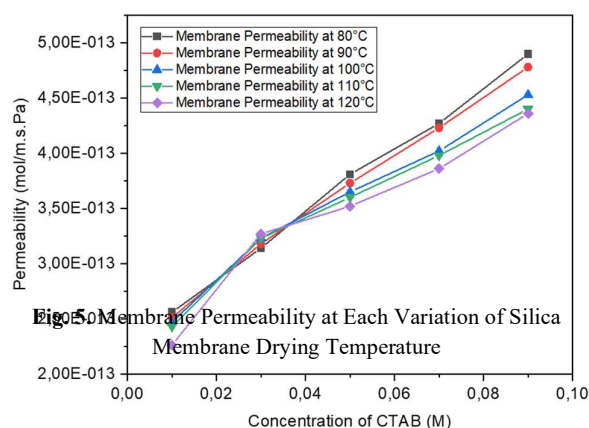
Fig. 5. Membrane Permeability at Each Variation of Silica Membrane Drying Temperature

Figure 5. illustrates the variation of CO_2 and CH_4 gas permeance with respect to CTAB concentration.

The results show that both CO_2 and CH_4 permeances increase from 0.01 M to 0.05 M CTAB, followed by a significant decrease at 0.09 M. The highest gas permeance was obtained at 0.05 M CTAB, suggesting that this concentration produced an optimal pore network within the silica layer. The increase in gas flux up to 0.05 M indicates that the membrane structure became more open due to effective micelle templating during the sol–gel process [13]. At higher CTAB concentration (0.09 M), the gas permeance decreased drastically. This phenomenon is attributed to overtemplating, where excessive surfactant concentration leads to irregular pore aggregation and partial blockage of transport channels, as supported by SEM observations. Such structural disorder limits gas diffusion and reduces the overall flux [12].
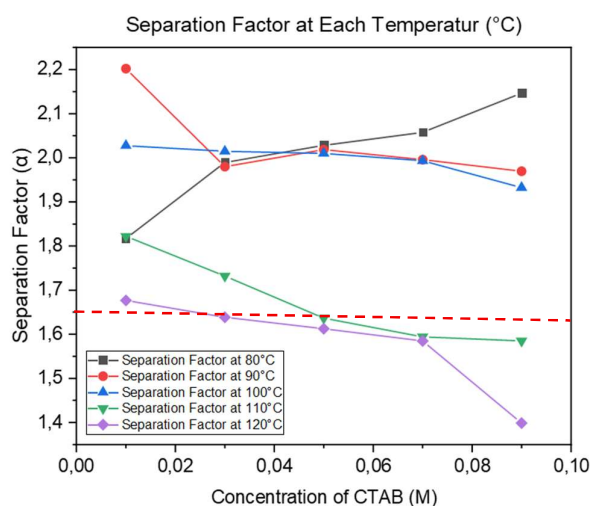

Fig. 6. Separation Factor Graph for Each Drying Temperature Variable

Figure 6 presents the CH_4/CO_2 selectivity of the membranes as a function of CTAB concentration. The selectivity increased with CTAB concentration, reaching approximately 3.21 at 0.05 M CTAB. This indicates that CH_4 permeated faster than CO_2, consistent with its lower molecular weight and smaller kinetic diameter (3.8 Å for CH_4 vs. 3.3 Å for CO_2). The observed trend agrees with the Knudsen diffusion mechanism, where lighter gases diffuse more rapidly through fine pores

$(\alpha(CH_4/CO_2),\text{Knudsen} = 1.66)$. The higher experimental selectivity ($3.21 > 1.66$) suggests that, in addition to Knudsen diffusion, structural factors such as improved pore connectivity and reduced defect density further enhance CH_4 transport through the silica network [17], [18]. The amorphous silica structure obtained at 0.05 M provides balanced porosity and stability, enabling higher gas permeance without sacrificing selectivity. Conversely, the overtemplated structure at 0.09 M generates disordered pore clusters that hinder separation efficiency [19]. In summary, the permeation data confirm that CTAB concentration significantly influences gas transport characteristics in silica membranes. An optimal balance between porosity and selectivity was achieved at 0.05 M CTAB, producing a membrane with high CH_4 flux and superior CH_4/CO_2 selectivity. These findings align with previous studies on sol–gel–derived silica membranes for biogas upgrading applications [12], [20].

3.4. Response Surface Methodology (RSM) Modeling of the Optimum Separation Factor for Bio-CNG Purification

The Response Surface Methodology (RSM) was employed to determine the optimum conditions of the separation factor (α) for CH_4/CO_2 separation using the Central Composite Design (CCD) in Design Expert software. The independent variables were CTAB concentration (A) and drying temperature (B), with 13 experimental runs summarized in Table 1. The highest separation factor (2.0282) was achieved at a CTAB concentration of 0.05 M and a drying temperature of 80 °C, indicating a synergistic interaction between surfactant structure-directing effect and controlled solvent removal during drying [21].

Table 1. Statistical Models with Separation Factor as The Response

Source	Sequel p-value	Lack of Fit p-value	Adjusted R^2	Predicted R^2	
Linear	0,0255	< 0,0001	0,4239	-0,1293	
2FI	0,0543	< 0,0001	0,5853	-0,4863	
Quadratic	**< 0,0001**	**< 0,0001**	**0,9817**	**0,8955**	Suggested
Cubic	0,0042	< 0,0001	0,9971	0,8618	Aliased

Table 2. Statistical Model of Silica Membrane Synthesis

Std	Run	Factor A: Concentration of CTAB	Factor B: Temperature	Separation Factor
1	10	0,01	80	1,8172
2	8	0,09	80	2,1467
3	6	0,01	120	1,6767
4	13	0,09	120	1,3987
5	9	0,01	100	2,0278
6	7	0,09	100	1,9324
7	4	0,05	80	2,0282
8	12	0,05	120	1,6126
9	2	0,05	100	2,0100
10	1	0,05	100	2,0100
11	3	0,05	100	2,0100
12	5	0,05	100	2,0100
13	11	0,05	100	2,0100

Table 3. Analysis of Variance (ANOVA) with Separation Factor as The Response

Source	Sum of Square	df	Mean Square	F- value	p- value	
Model	0,5400	5	0,1080	130,00	< 0,0001	Significant
A-Concentration of CTAB	0,0003	1	0,0003	0,3867	0,5538	
B-Temperature	0,2834	1	0,2834	341,21	< 0,0001	
AB	0,0923	1	0,0923	111,07	< 0,0001	
A²	0,0055	1	0,0055	6,65	0,0366	
B²	0,1154	1	0,1154	138,92	< 0,0001	
Residual	0,0058	7	0,0008			
Lack of Fit	0,0058	3	0,0019			
Pure Error	0,0000	4	0,0000			
Cor Total	0,5458	12				

The statistical modeling results summarized in Table 1. and Table 2. reveal that the quadratic model was significant (F = 130.00, p < 0.0001) with an R^2 of 0.9893 and an adjusted R^2 of 0.9817. This indicates that 98.93% of the data variability can be explained by the model, suggesting high reliability and predictive capability. The temperature factor (B) and the interaction term (A × B) significantly affected α (p < 0.0001), whereas the linear CTAB effect was less pronounced. The negative quadratic coefficients for both variables (A² and B²) imply non-linearity and the presence of an optimum region for α [22]. The fitted quadratic equations derived from coded and actual factors were:

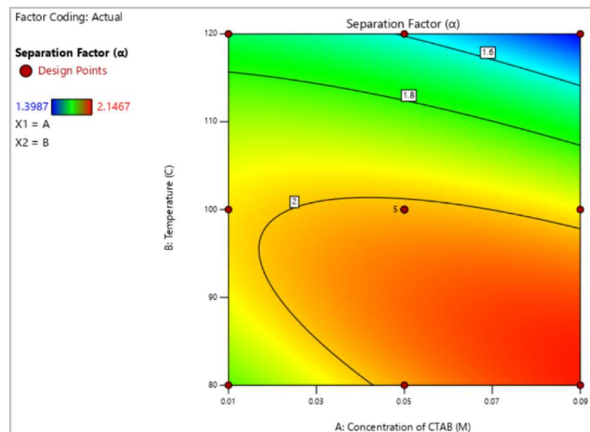$$Separation\ Factor = +6,42 - 0,185\ A + 0,297\ B + 0,212\ A*B - 0,221\ A^2 - 0,338\ B^2$$

$$Separation\ Factor = -28,765 + 0,6124\ CTAB + 0,0847\ Temp. + 0,00321\ CTAB*Temp. - 0,0376\ CTAB^2 - 0,00089\ Temp.$$
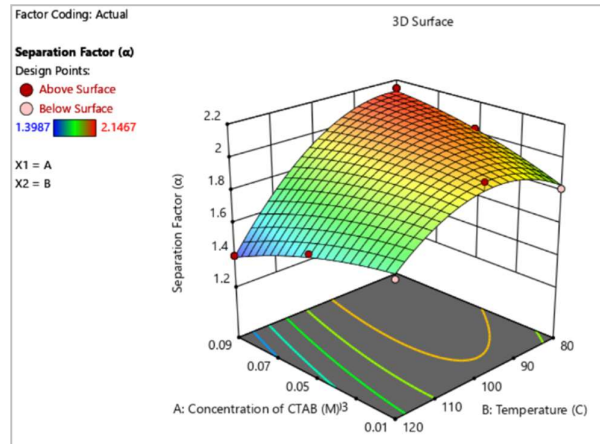
Where :

A = Concentration of CTAB, M

B = Temperature, ºC

These models confirm that both variables exhibit a strong interaction influencing the separation factor response. As shown in Figure 7, the contour plot demonstrates the optimum region (red area) at CTAB ≈ 0.05 M and temperature ≈ 105 °C, corresponding to the highest α of 2.1467. Figure 8, the 3D surface plot, further confirms the curvature of the response surface, emphasizing non-linear interactions between A and B [23], [24]

Fig. 7. Contour Plot with Separation Factor as The Response

At lower temperatures (< 90 °C), the separation factor decreases due to incomplete solvent removal, while excessive drying (> 110 °C) leads to pore collapse and reduced selectivity [25]. These findings are consistent with Montgomery's design principles and similar sol–gel silica membrane optimizations reported by Baskaran et al [23] and Yoshimoto et al [17]. Although the RSM

model predicted an optimum α of approximately 2.15 under the combined conditions of 0.05 M CTAB and a drying temperature of 105 °C, the subsequent experimental gas permeation test yielded a slightly higher value of 3.21. This deviation is reasonable, given that the RSM prediction is based on interpolated statistical data from a limited design space, whereas the final gas permeation measurement reflects the actual membrane performance after complete microstructural stabilisation. The experimentally observed enhanced α suggests that additional factors, such as improved pore interconnectivity, densification during post-drying, and partial surface diffusion, contributed to the higher CH_4/CO_2 selectivity beyond the RSM's quadratic approximation.

Fig. 8. 3D Interaction Plot of Separation Factor, Concentration of CTAB, and Temperature

Therefore, the quadratic RSM model effectively predicts the relationship between synthesis parameters and membrane performance. The combination of 0.05 M CTAB and a drying temperature of 105 °C was found to yield the highest selectivity and system stability, demonstrating the reliability of the developed silica membrane for bio–CNG upgrading applications [8].

4. CONCLUSION

Silica membranes were successfully synthesized on α–alumina substrates via a surfactant-assisted sol–gel route using CTAB as a pore-directing agent for bio–CNG purification. The combined analyses of morphology, structure, and gas permeation revealed that CTAB concentration played a crucial role in controlling pore uniformity, surface homogeneity, and separation behavior. The membrane prepared with 0.05 M CTAB exhibited the most favourable characteristics, including uniform Si distribution, an amorphous silica structure, and a balanced pore network, yielding the highest CO_2/CH_4 separation factor of 3.21. Further optimisation using Response Surface Methodology (RSM) confirmed that CTAB concentration, ageing time, and drying temperature significantly affected the separation performance, yielding an optimal predicted separation factor of 3.27 at 0.051 M CTAB, 36 h ageing, and 121 °C. These findings demonstrate that precise surfactant and thermal control during the sol–gel synthesis effectively tailor membrane microstructure for enhanced CO_2/CH_4 separation, offering a promising pathway for efficient and sustainable bio–CNG upgrading applications.

REFERENCES

[1] A. D. W. M. Sidik, H. Lumbantobing, B. Indrawan, E. Y. Putra, Y. Imamulhak, and R. Rinaldi, "Studi Potensi Pemanfaatan Energi Baru Terbarukan (EBT) untuk Mendukung Sistem Ketenagalistrikan di Wilayah IKN," *J. Sist. Komput. dan Kecerdasan Buatan*, vol. 6, no. 2, pp. 137–144, 2023.

[2] Badan Pusat Statistik, "Neraca Energi Indonesia 2018-2022," Badan Pusat Statistik. [Online]. Available: https://www.bps.go.id

[3] A. Wijono, "Dampak Pengurangan Emisi Gas Rumah Kaca Pada Pemanfaatan POME Untuk Pembangkit," in *Prosiding Semnastek*, 2017, pp. 1–2.

[4] A. A. Damayanti, Z. N. Fuadina, N. N. Azizah, Y. Karinta, and I. K. Mahardika, "Pemanfaatan Sampah Organik Dalam Pembuatan Biogas Sebagai Sumber Energi Kebutuhan Hidup Sehari-Hari," *Eksergi J. Tek. Energi*, vol. 17, no. 3, pp. 182–190, 2021, doi: 10.32497/eksergi.v17i03.2803.

[5] W. K. Setiawan and K. Y. Chiang, "Silica applied as mixed matrix membrane inorganic filler for gas separation: A review," *Sustain. Environ. Res.*, vol. 1, no. 1, 2019, doi: 10.1186/s42834-019-0028-1.

[6] D. Andriani *et al.*, "A review on biogas purification through hydrogen sulphide removal," in *IOP Conference Series: Earth and Environmental Science*, Institute of Physics Publishing, Jun. 2020, pp. 1–11. doi: 10.1088/1755-1315/483/1/012034.

[7] M. A. Pizzoccaro-Zilamy *et al.*, "New Generation of Mesoporous Silica Membranes Prepared by a Stöber-Solution Pore-Growth Approach," *ACS Appl. Mater. Interfaces*, vol. 11, no. 20, pp. 18528–18539, May 2019, doi: 10.1021/acsami.9b03526.

[8] P. D. Sutrisna, R. P. Hadi, J. Siswanto, and G. J. Prabowo, "The co2/ch4 separation potential of zif-8/polysulfone mixed matrix membranes for biogas upgradation process," *Int. J. Renew. Energy Dev.*, vol. 10, no. 2, pp. 213–219, 2020, doi: 10.14710/ijred.2021.33118.

[9] Y. Han, L. Zhang, and W. Yang, "Synthesis of Mesoporous Silica Using the Sol–Gel Approach: Adjusting Architecture and Composition for Novel Applications," Jun. 01, 2024, *Multidisciplinary Digital Publishing Institute (MDPI)*. doi: 10.3390/nano14110903.

[10] F. F. Pitard, *Theory of Sampling and Sampling Practice Third Edition*. London: CRC Press, 2019.

[11] R. J. R. Uhlhorn, M. H. B. J. Huis In't Veld, K. Keizer, and A. J. Burggraaf, "High permselectivities of microporous silica-modified y-alumina membranes," *J. Mater. Sci. Lett.*, vol. 8, pp. 1135–38, 1989.

[12] Y. Gao, R. Sun, L. Yu, and W. Wang, "Facile preparation of hierarchical mesoporous silica microspheres with tunable porous structure and particle sizes," *Ceram. Int.*, vol. 49, no. 2, pp. 3030–3040, 2023, doi: https://doi.org/10.1016/j.ceramint.2022.09.287.

[13] N. A. Z. Kahlib, F. D. M. Daud, M. Mel, A. L. N. Hairin, A. Z. A. Azhar, and N. A. Hassan, "Fabrication of silica ceramic membrane via sol-gel dip-coating method at different nitric acid amounts," in *IOP Conference Series: Materials Science and Engineering*, Institute of Physics Publishing, Jan. 2018. doi: 10.1088/1757-899X/290/1/012042.

[14] L. P. Singh *et al.*, "Sol-Gel Processing of Silica Nanoparticles and Their Applications," *Adv. Colloid Interface Sci.*, vol. 214, pp. 17–37, 2014, doi: 10.1016/j.cis.2014.10.007.

[15] M. Iqbal, K. K. Dewa, M. Dyah, S. Suprihatin, and N. A. Fauziyah, "Pengaruh pH dan CTAB (Cetyl Trimethyl Ammonium Bromida) terhadap Morfologi Silika," *J. Fis. Unand*, vol. 13, no. 3, pp. 433–438, 2024, doi: 10.25077/jfu.13.3.433-438.2024.

[16] A. Zakeri Siavashani, M. Haghbin Nazarpak, F. Fayyazbakhsh, T. Toliyat, S. J. P. McInnes, and M. Solati-Hashjin, "Effect of amino-functionalization on insulin delivery and cell viability for two types of silica mesoporous structures," *J. Mater. Sci.*, vol. 51, no. 24, pp. 10897–10909, Dec. 2016, doi: 10.1007/s10853-016-0301-1.

[17] Y. Yoshimoto *et al.*, "Gas Adsorption and Diffusion Behaviors in Interfacial Systems Composed of a Polymer of Intrinsic Microporosity and Amorphous Silica: A Molecular Simulation Study," *Langmuir*, vol. 38, no. 24, pp. 7567–7579, 2022.

[18] A. Nijmeijer, "Hydrogen-Selective Silica Membranes for Use in Membrane Steam Reforming," University of Twente, 1999.

[19] Y. Fan, W. Yu, A. Wu, W. Shu, and Y. Zhang, "Recent progress on CO2 separation membranes," *RSC Adv.*, vol. 14, no. 29, pp. 20714–20734, Jul. 2024, doi: 10.1039/d4ra00444b.

[20] H. Purwaningsih, Y. Ervianto, V. M. Pratiwi, and D. Susanti, "Effect of Cetyl Trimethyl Ammonium Bromide as Template of Mesoporous Silica MCM-41 from Rice Husk by Sol-Gel Method," *IOP Conf. Ser. Mater. Sci. Eng.*, vol. 515, no. 012051, pp. 1–9, 2019, doi: 10.1088/1757-899X/515/1/012051.

[21] S. Singla, N. P. Shetti, S. Basu, K. Mondal, and T. M. Aminabhavi, "Hydrogen production technologies - Membrane based separation, storage and challenges," *J. Environ. Manage.*, vol. 302, p. 113963, 2022, doi: https://doi.org/10.1016/j.jenvman.2021.113963.

[22] D. C. Montgomery, *Chapter 13: Response Surface Methods and designs*. 2017.

[23] K. Baskaran *et al.*, "Sol-gel derived silica: A review of polymer-tailored properties for energy and environmental applications," *Microporous Mesoporous Mater.*, vol. 336, no. December 2021, p. 111874, 2022, doi: 10.1016/j.micromeso.2022.111874.

[24] S. Hosseini, I. Shiryanpour, A. Alibak, M. Fattahi, and A. Hassanvand, "Modeling of the Effect of Nanoparticles on CO2/CH4 Selectivity of Poly (4-methyl-1-pentene)-Based Mixed Matrix Membranes," *Arab. J. Sci. Eng.*, vol. 50, pp. 1–11, Jun. 2024, doi: 10.1007/s13369-024-09216-x.

[25] Y. Yang, Q. Chang, Z. Hu, and X. Zhang, "A comparative study on the addition methods of TiO2 sintering aid to the properties of porous alumina membrane support," *Membranes (Basel).*, vol. 8, no. 3, Sep. 2018, doi: 10.3390/membranes8030049.